Journal of Hazardous Materials 159 (2008) 412–419

Contents lists available at ScienceDirect

Journal of Hazardous Materials

journal homepage: www.elsevier.com/locate/jhazmat

Kinetics and modified clay thermodynamic from the Brazilian amazon region for lead removal

Denis L. Guerra*, Claudio Airoldi

Instituto de Química, Universidade Estadual de Campinas UNICAMP, Caixa Postal 6154, 13084-971 Campinas, São Paulo, Brazil

ARTICLE INFO

Article history:
Received 6 January 2008
Received in revised form 9 February 2008
Accepted 12 February 2008
Available online 17 February 2008

Keywords:
Ceramic
Surface property
Inorganic compound
Thermodynamic property

ABSTRACT

Modified Brazilian smectite-bearing clay samples displayed ability for lead adsorption. The structure modification of smectite were obtained through pillaring process and functionalization with [3-(2-aminoethylamino)propyl]trimethoxysilane. The chemical modification process increases the basal spacing of the natural smectite from 1.354 to 2.364 nm. The Langmuir model was fitted to experimental data in linear regression. Kinetic studies showed an equilibrium adsorption time of 700 min on the modified clay. The experimental data were correlated with two distinct kinetic models were used: (i) external mass transfer diffusion and (ii) intraparticular mass transfer diffusion. However, the intraparticle mass transfer diffusion model gave a better fit to these experimental data. The energetic effects caused by lead interactions were determined through calorimetric titration at the solid–liquid interface and gave a net thermal effect that enabled the calculation of the exothermic values and the equilibrium constant.

1. Introduction

The presence of heavy metals in the environment is a general concern of mankind due to their inherent acute toxicity, mainly when the content produced from industries is discharged as aqueous effluents [1–22]. The health hazards results from the presence of leads in industrial wastewaters are of extreme concern to the public, government and industries for about two decades now. The deleterious effects of lead on neurobehavioral development and brain cell function have been investigated [11].

The heavy metals in aqueous medium can be removed by several processes, such as ion exchange, precipitation and adsorption [2]. Development of low cost adsorbents of easy application, regeneration and reuse are desirable properties associated with adsorption from the liquid phase, as an interesting process for manipulating contaminated water [13]. Various common and non-usual adsorbent materials have been tried for metal ion removal from aqueous solutions. Among these available materials, silica gel [8,9], pillared clay of the smectite 2:1 group [2,3], exfoliated and intercalated kaolinite [10], blast furnace slag [11], etc., are examples of such applications.

The aim of the present investigation is to study the physical–chemical properties of smectite (montmorillonite type) modified through of the pillaring and organofunctionalization process, the synthetic procedure based on $Al_{13}O_4(OH)_{24}(H_2O)_{12}{}^{7+}/ZrOCl_2{\cdot}8H_2O$ mixed pillarization process and organofunctionalization with sylane [3-(2-aminoethylamino)propyl] trimethoxysilane (APTS). The Langmuir adsorption isotherm model was applied in order to fit the experimental data after lead (II) adsorption in linear regression. The kinetics correlated with the external mass transfer diffusion model for the first stage while the intraparticle mass transfer diffusion model was adjusted to the second stage of adsorption. The energetic effect caused by divalent metal (Pb^{2+})/smectite (in form natural and chemically modified) interaction was determined through calorimetric titration.

2. Experimental

2.1. Raw material

Clay samples used in this investigation were collected from the Sena Madurera area, Acre State, northern region of Brazil. The natural smectite sample, named CL with less than 2 μm particles was separated by sedimentation. The cation-exchange capacity (CEC) was measured in order to evaluate the potential use of those clays for pillarization and organofunctionalization process. The exchange was followed by using ammonium acetate method with concentration of 2.0 mol dm^{-3} at pH 8.0 and room temperature, which obtained result, gave 1.55 mmol g^{-1} on an air-dried basis. The value of CEC can be attributed to presence of fractions kaolinite and goethite in natural sedimentation sample, kaolinite and goethite are mineral clays common in amazon soil due to the fact that the Amazon climate is normally warm-humid, causing acidic lixiviation

* Corresponding author. Tel.: +55 1933429407; fax: +55 1933429407.
E-mail address: dlguerra@iqm.unicamp.br (D.L. Guerra).

0304-3894/$ – see front matter © 2008 Published by Elsevier B.V.
doi:10.1016/j.jhazmat.2008.02.032

in soils, conditions that are favorable to interstratified smectite formation [2,3].

The samples were dried at 333 K to have humidity in the 12–15% range, and were ground and passed through a USS sieve no. 200 (0.074 mm). Part of the smectite clay was dispersed in doubly deionised water for several hours and was further purified using an established method [8–10]. Powder X-ray diffraction identified the presence of this smectite clay using conventional sample preparation procedures, such as air-dried oriented mounts, ethylene glycol solvation and heating at 573 and 773 K [9].

2.2. Purification of clay samples

Wet sedimentation were soaked in 50.0 dm^3 of distillated water and disaggregated for 24 h in ultrasound. After removing of sand fraction (>63 μm Ø) with wet sieve, supernatant of suspension contains water were removed by centrifuging at 3400 rpm for 1.0 h. For deflocculation of particles, 0.001 mol dm^{-3} sodium hexametaphophate were added. At this time, three dispersing agents, 1% sodium polyphosphate [8], 0.005 mol dm^{-3} sodium pyrophosphate [9] and 0.005 mol dm^{-3} sodium hexametaphophate [10], were attempted to compare effectiveness for particle separation and influence for clay minerals. Silt fraction (2–36 μm Ø) and clay fraction (<2 μm Ø) were separated by centrifuging at 700 rpm three times using modified Stoke's law [10]. At each cycle, to correct centrifuging duration, we measured water temperature and distance to sink 2 μm particles. All extracted clay fraction were gathered in one tube and then washed by distillated water for three times to removed dispersion agent.

2.3. Characterization of smectite samples

The natural smectite sample was analyzed with a induced coupled plasma-optical emission spectrometry (ICP-OES) instrument, using an ARL 34000 instrument.

X-ray powder diffraction (XRD) patterns were recorded in a Philips PW 1050 diffractometer using CuKα (0.154 nm) radiation in the region between 2 at 65° (2θ) at a speed of 2° per min and a step of 0.050°.

The amount of lead adsorbed was determined by the difference between the initial concentration in aqueous solution and that found in the supernatant by using an ICP-OES PerkinElmer 3000DV instrument. For each experimental point, the reproducibility was checked by at least one duplicate run. X-ray powder diffraction (XDR) patterns were recorded on a Philips PW 1050 diffractometer using CuKα (0.154 nm) radiation in the region between 2 at 65° (2θ) at a speed of 2° per min and steps of 0.050°.

The nuclear magnetic resonance spectra of modified smectite were obtained on an AC 300/P Bruker spectrometer at 298 ± 1 K at 59.6 Mhz for silicon. A pulse repetition time of 3 s and contact time of 3 ms were used for $^{29}Si\{^1H\}$ CPMAS experiments.

The carbon, nitrogen and hydrogen contents were determined on a PerkinElmer 2400 Series II microelemental analyzer, and at least two independent determinations were performed for each sample.

2.4. Synthesis of the pillared clays (PILC)

A molar ratio of OH/Al = 2 was prepared by slow addition of 0.20 mol dm^{-3} NaOH to a 0.20 mol dm^{-3} aqueous $AlCl_3 6H_2O$ solution. The initial basic solution was added dropwise to the aluminum solution, which was maintained under vigorous stirring at 333 K [2].

The zirconium solution was prepared by adding appropriate volumes of 0.10 mol dm^{-3} aqueous $ZrOCl_2 8H_2O$ solution directly to aqueous clay suspension at room temperature with vigorous stirring [12].

The mixed polymeric Al/Zr solution was added dropwise to a suspension of 5.0% of natural clay sample CL in a mixture of deionized water and ethanol. The final solution containing polymeric ions (Al, Zr) and natural clay sample was filtered and washed with deionized water. The samples were calcinated at 723 and 873 K for 2 h [12]. These materials were named Al/Zr-PILC.

2.5. Organofunctionalization

5.0 g of pillared smectite Al/Zr-PILC suspended in xylene (120.0 cm^3) was refluxed and mechanically stirred for 60 min under dry nitrogen. To this suspension [3-(2-aminoethylamino)propyl]trimethoxysilane $(CH_3O)_3Si(CH_2)_3NHCH_2CH_2NH_2$ (Aldrich) (7.5 cm^3) was added dropwise. The mixture was refluxed for another 30 h, centrifuged and washed with water, followed by methanol and acetone. The resulted material was dried at 353 K [12]. The resulting sample was called Al/Zr-$PILC_{APT}$.

The thermal effects from lead cations interacting on natural and modified smectite samples were followed in an isothermal LKB 2277 microcalorimetric system. A sample of approximated 10.0 mg of natural and modified smectite were using in calorimetric titration. After calorimetric baseline stabilization, the 20.0 cm^{-3} metal cations, was individually added to the vessel by means of microsyringe coupled to a stainless steel needle. In individual titration, the thermal effect caused by the reaction was recorded after each addition of the titration [23–25].

2.6. Adsorption

Samples of about 60 mg of the Al/Zr-$PILC_{APT}$ suspended in 20.0 cm^3 of aqueous solution containing lead at 298 ± 1 K were used to investigate the adsorption process. Firstly, natural and modified adsorption samples was evaluated by varying the pH in the 1.0–6.0 range with addition of 0.10 mol dm^{-3} of nitric acid or 0.10 mol dm^{-3} sodium hydroxide.

Samples of about 60 mg of the Al/Zr-$PILC_{APT}$ were suspended in an aqueous solution containing lead cation with continuous orbital stirring for the adsorption process at 298 ± 1 K and pH 6.0, with a contact time of 700 min, enough to reach the plateau of the complete isotherm. Identically, isotherms of concentration versus time were obtained using the batch method [14]. The number of moles adsorbed per gram (N_f) is calculated by the difference between the initial (N_i) and the remaining moles of Pb(II) in the supernatant (N_s) divided by the mass (m) of the compound used the Eq. (1) [2,14].

$$N_f = \frac{N_i - N_s}{m} \quad (1)$$

The number of moles cation adsorbed (N_f) increased with time (t) as a function of the concentration in the supernatant (C_s). From this procedure the plateau related to total saturation of the acid centers in the layered structure was obtained.

The most commonly used isotherms are those related to Langmuir, which was originally derived for gas adsorption on planar surfaces such as glass, mica and platinum. For this adsorption model a quantity q_i of an adsorbate, where i related to the equilibrium solution concentration of the adsorbate c_i, is adjusted to K_L and b parameters. The plateau of the isotherm enables K_L determination by measuring the adsorbate on surface. The values of b is the upper limit for q_i and represents the maximum adsorption of i determined by the number of reactive surface sites by converting Eq. (2) into its linear form [2,14]:

$$\left[\frac{C_s}{N_f}\right] = \left[\frac{1}{K_L b}\right] + \left[\frac{C_s}{b}\right] \quad (2)$$

Table 1
Elemental analyses of natural clay (CL) and modified clay Al/Zr-PILC$_{APT-T}$ samples

Sample	SiO_2 (%)	Al_2O_3 (%)	CaO (%)	Na_2O (%)	K_2O (%)	Fe_2O_3 (%)	MgO (%)	ZrO_2 (%)
CL	58.78	16.89	3.68	1.31	3.92	6.1	3.97	–
Al/Zr-PILC$_{APT-723}$	58.78	17.71	1.03	0.71	2.02	5.8	3.94	2.20
Al/Zr-PILC$_{APT-873}$	58.78	17.65	1.08	0.19	2.13	5.6	3.92	2.11

Then, $c_i/q_i = C_s/N_f$ and the so-called distribution coefficient K_L, can be plotted against q_i. If the Langmuir equation can be applied, the measured data should fall on a straight line with slope giving K_L and the intercept K_L b values, $1/K_L$ b being the angular and $1/b$ the linear coefficients [14].

3. Results and discussion

3.1. Characterization clay sample

Elemental analyses from the coupled plasma-optical emission spectrometry (ICP-OES) instrument for the original and chemically modified clay samples gave the results listed in Table 1. These values are consistent with smectite, with aluminum being the major clay mineral contained in the structure, followed by calcium, potassium, magnesium and sodium, in agreement with the attachment of the aluminum and zirconium ions in the original smectite structure. The structural formula of smectite original sample was calculated through of the chemical analysis, this formula is represented by:

$$CL: (Na_{0.17}K_{0.38}Ca_{0.26})(Al_{1.15}Mg_{0.13}Fe_{0.30}{}^{3+})(Si_{3.85}Al_{0.15}O_{10})(OH)_2 \quad (3)$$

The resulted formula can be represented a smectite montmorillonite. The clay presented four atoms of silicon in the tetrahedral structure, suggesting two hypotheses, the presence of silicon in amorphous form in the matrix and possibility of isomorphic substitution in the crystalline net of matrix [19].

The X-ray powder diffraction technique confirmed an expansion of the original smectite to thermally stable d_{001} spacing from 1.354 to 2.364 and 20.067 nm for Al/Zr-PILC$_{APT-723}$ and Al/Zr-PILC$_{APT-873}$, respectively. These d_{001} peaks demonstrated structural modified arrangement in the matrices. Such clays are very stable up to the high temperatures of calcinations, reaching 873 K, as shown in Fig. 1. The Al/Zr-PILC$_{APT-723}$ clay presented a lager d_{001} value compared to other one, and was chosen for the kinetic and thermodynamic investigation. According to the results of matrix d_{001} expansion obtained by Ruiz et al. [26] in adsorption investigation with inorganic–organic hybrids derived from lamellar acidic kenyaite, these matrices were intercalated by 3-aminopropyltriethoxysilane, *N*-propyldiethilenetrimethoxysilane and bis[3-(trietoxysilyl)propil]tetrasulfide, by expanding the interlayer distance of 1633 pm to 1933, 1847 and 1828 pm.

Fig. 2 shows ^{29}Si-MAS/NMR spectra of the modified smectite samples in two different calcination temperatures. In these spectrum was observed peaks at −57.62 ppm (T^2), −68.17 ppm (T^1), −79.23(Q^2) and −91.62 ppm (Q^3) [15]. Clear evidence of alkoxysilane reaction with the available groups in the pillared smectite (Al/Zr-PILC) by the ^{29}Si MAS/NMR spectra, the external part of pillars and internal surface of smectite, which were exposed with pillarization process are relatives groups into smectite structure. The peaks T^2 and T^3, near ∼−50 to −60 ppm, in Al/Zr-PILC are attributed to the Si atoms of the grafted APTS molecules. The signals for APTS silylated on silica appeared in the range −49 to −68 ppm depending upon bonding type [16]. Si signals for APTS grafted on layered silicates was also appeared at ∼−56 to −65 ppm. According to the results obtained by Park and Kwon [16] in study with H-montmorillonite (Yaguri-Japan) was modified by interlayer surface silylation using 3-aminopropyltriethoxysilane and dodecylamine. The increase in the relative intensity of Q^3 (∼−96 ppm) for Q^2 (∼−90 ppm) appearance of T^2 (∼−50 ppm) and T^3 (∼−60 ppm) signals was attributed to the grafting of intercalated agent to the interlayer surface silanol groups.

The successful immobilization gave elemental analyses for the silylated surface as listed in Table 2. The amount incorporated was calculated based on the amount of nitrogen and carbon existents in modified montmorillonite samples. Based on the analytical data for both nanocompounds, the density of these pendant organic molecules immobilized on the montmorillonite layer of the phyllosilicate can be calculated. Thus, the sililant agents grafted onto

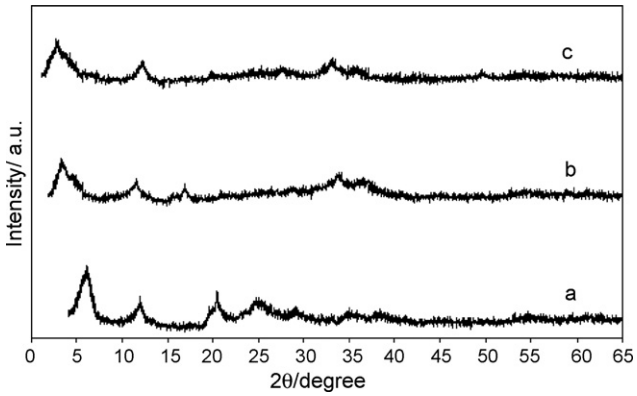

Fig. 1. X-ray patterns of natural CL (a) and Al/Zr-PILC$_{APT}$ clays calcinated at (b) 723; (c) 873 K.

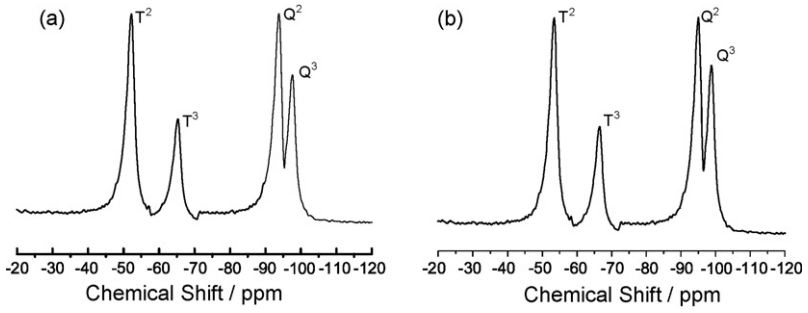

Fig. 2. ^{29}Si MAS NMR spectra of modified smectite samples: Al/Zr-PILC$_{APT-723}$ (a) and Al/Zr-PILC$_{APT-873}$ (b).

Table 2
Percentages of carbon (C), hydrogen (H) and nitrogen (N) obtained through elemental analysis of the inorganic–organic hybrids, density (d) of the pendant molecules bonded on silicon layers

Sample	C (%)	H (%)	N (%)	d (mmol g^{-1})
Al/Zr-PILC$_{APT-723}$	15.43 ± 0.11	2.48 ± 0.01	6.96 ± 0.02	9.12 ± 0.04
Al/Zr-PILC$_{APT-873}$	14.89 ± 0.17	2.44 ± 0.02	7.09 ± 0.02	9.18 ± 0.08

montmorillonite structure gave an amount of 9.12 ± 0.04 mmol g^{-1} (Al/Zr-PILC$_{APT-873}$) and 9.18 ± 0.08 mmol g^{-1}(Al/Zr-PILC$_{APT-723}$).

3.2. Kinetics of adsorption

The pH of the aqueous solution is an important controlling parameter in the adsorption process. The influence of the pH values on concentration by natural and modified clays, represented by the number of moles adsorbed, N_f, is plotted in Fig. 3, showing that the exchange of metal ions strongly decreases with the acidity of the solution. Obviously, a pH value 6.0 is optimal for the adsorption of metal ions. Exchange experiments at higher than 6.0 were not carried out due to the risk of hydrolysis.

The results obtained with Pb(II) cations at pH 6.0 and controlled temperature (298 ± 1 K), as a function of concentration and time, are shown in Figs. 4 and 5, respectively. This behavior clearly demonstrated similar increases adsorption with the increases in the lead concentration up to a contact time of 700 min. The same condition for adsorption as a function of concentration of the supernatant is shows in Fig. 4. The experimental data applied to the Langmuir model of adsorption enabled the calculation of the parameters listed in Table 3. These values are in agreement with this possible model of adsorption and they could be used to explain the significant capacity of the modified matrices to quantify the adsorption. This quantification of the adsorption capacities of Pb(II) ions on the inorganic structure can be evaluated and from it the possibility to obtain the constant, which expresses the bonding energy [11].

Metal bonding formation with the internal pillared spices and APTS in the clays is favored, by increasing the pillar wall surfaces of the original smectite structures, besides the external part of the pillars. This complete process of metal/clay bonding is governed by the microenvironment around those pillar bridges, which are usually covered by basic centers (OH groups) and reactive centers of APTS ions (NH groups) Scheme 1. These coordinating centers are formed as accessories in the pillars, due to the appearance of hydroxyl groups that still exist on the surfaces, mainly in hydration

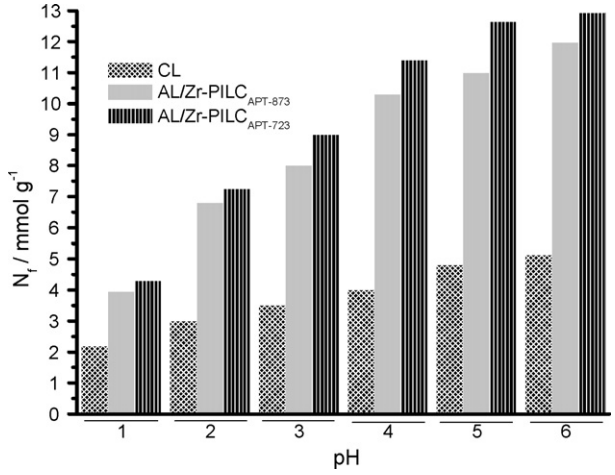

Fig. 3. Effect of pH on lead adsorptions from aqueous solution for 3.0 g dm^{-3} clay, with lead concentration 60.0 mg dm^{-3}, at 298 ± 1 K.

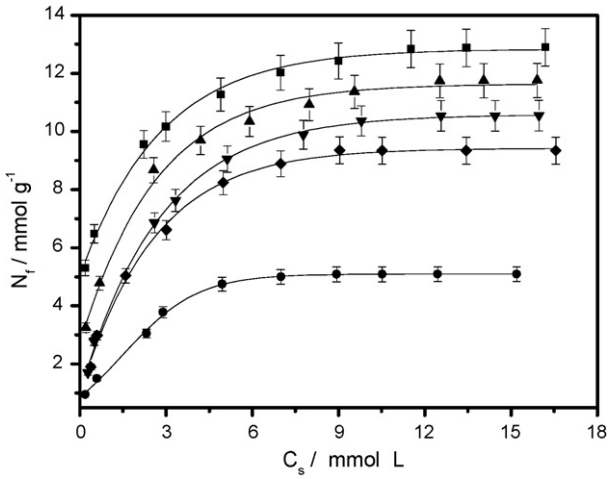

Fig. 4. Adsorption of lead on 3.0 g dm^{-3} of clay or modified Al/Zr-PILC$_{APT}$ (temperature of calcination = 723 K) clay, at pH 6.0 and controlled temperature 298 ± 1 K. Lead concentration 60.0 mmol dm^{-3} on natural (●), and 100.0 (■), 60.0 (▲); 20.0 (▼) and 10.0 mmol dm^{-3} (♦) on modified clay.

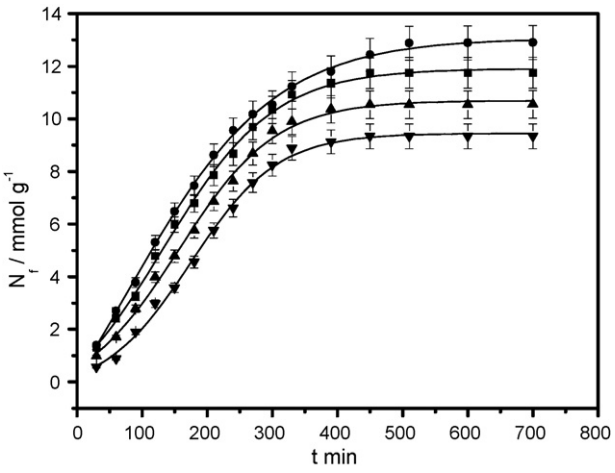

Fig. 5. The effect of contact time on the Al/Zr-PILC$_{APT}$ (temperature of calcination = 723 K) for 3.0 g dm^{-3} of clay, at pH 6.0 and controlled temperature 298 ± 1 K for Pb(II): 100.0 (●), 60.0 (■); 20.0 (▲) and 10.0 mmol dm^{-3} (▼).

of the internal structure and NH groups anchored in internal surface and pillars. Thus, the positioning and amount of hydroxyl and NH groups in outer regions, as in lamellae borders or central structures, control chemisorption processes.

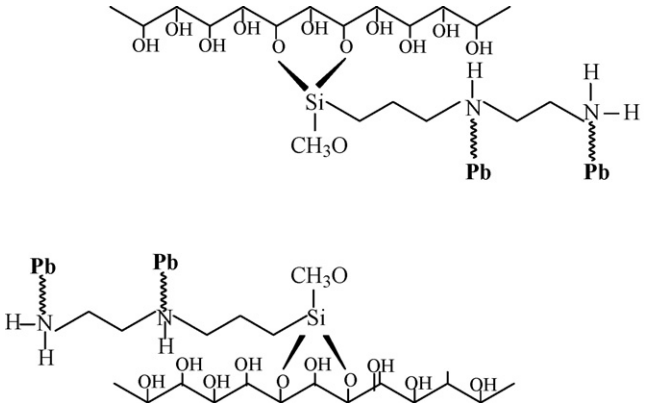

Scheme 1. Schematic representation of resulting structure of modified clay in the adsorption of lead cation.

Table 3
External mass transfer diffusion (k_f) and intraparticular mass transfer diffusion (D_i) coefficients for the adsorption of Pb(II) onto Al/Zr-PILC$_{APT}$ with calcination temperature of 723 K (clay 3.0 g dm^{-3}, pH 6.0, controlled temperature 298 ± 1 K)

[Pb] (mmol dm^{-3})	$K_L \times 10^{-3}$	r^2	$D_i \times 10^{-15}$ (m^2 s^{-1})	r^2	$k_f \times 10^{-7}$ (cm s^{-1})	r^2
100	14.58 ± 0.15	0.998	12.99 ± 0.11	0.998	3.65 ± 0.13	0.999
60	12.21 ± 0.17	0.997	10.65 ± 0.12	0.999	2.97 ± 0.16	0.999
20	11.52 ± 0.17	0.999	7.46 ± 0.12	0.998	0.69 ± 0.17	0.998
10	10.91 ± 0.17	0.998	5.46 ± 0.14	0.999	0.05 ± 0.18	0.997

Natural and modified clays showed identical behavior for Pb(II) uptake with time, with a rapid increase up to 180 min and then a slower increase as the equilibrium is reached, with higher values for the modified clays in comparison with the original one, as shown in Fig. 5. For all cases, the Pb(II) uptake became almost constant after 500 min, which can be considered reaching near equilibrium conditions, established by a plateau. During the experimental procedure the initial and final pH values were measured without changing in value. The presence of pillars and APTS molecules in the clay structure has resulted in a higher uptake of Pb(II) for the same interaction time, this behavior can be attributed to the increase in the number of equivalent adsorption sites.

Some parameters influence the kinetics of reaction, such as temperature and concentration [17–19]. These provided information about the mechanism of adsorption that can give important features related to the efficiency of the process of adsorption. For this investigation two distinct kinetic models were used: (1) external mass transfer diffusion and (2) intraparticular mass transfer diffusion. The charge on Pb(II) in such concentrations with the respective time for the first stage of adsorption may be related to the liquid solid mass transfer coefficients (k_f), obtained through the following equation [15,17]:

$$\ln\left[\left(\frac{C_T}{C_o}\right) - \left(\frac{1}{1+mK_L}\right)\right] = \ln\left[\frac{mK_L}{1+mK_L}\right] - \left(\frac{1+mK_L}{mK_L}\right) k_f S_s t \quad (4)$$

$$S_s = \frac{6C_o}{dp_s}(1-\varepsilon) \quad (5)$$

where C_T is the concentration of Pb(II) at time t (min), C_o is the initial concentration of Pb(II) (mmol dm^{-3}), K_L and b are constants obtained by linear regression of the experimental curves, m is the mass of the adsorbent per unit volume of particle-free adsorbate solution (g dm^{-3}), S_S is the outer surface of the adsorbent per unit volume of the particle-free slurry (cm^{-1}), dp_s is solid density (g cm^{-1}) and ε is particle voidage. The values of k_f were calculated from the slope and the intercepts of the plots of $\ln[(C_T/C_0) - (1/1+mK_L)]$ versus time (t) for various concentrations and temperatures using the least square method and the results are presented in Table 3 and Fig. 6. It was observed that k_f values are affected by the initial concentration with a gradual decrease, which indicates cation adsorption by modified clay, independent of the calcination temperature, increasing with cation concentration.

As observed, the k_f values increased with temperature, suggesting that the adsorption is thus faster at higher temperature, as shown in Table 3. It is clear from these values that the velocity of transport of the adsorbate from the liquid to solid phase is rapid enough to use modified clays for the treatment of Pb(II) wastewaters.

Due to the porous nature of the adsorbent, intraparticular mass transference diffusion is expected to be the rate-limiting step. In this study, a kinetic model was chosen to describe the kinetic data [17–21]. The relationship between the uptake amount and sorption time for moderate and longer times given by the following equation:

$$f\left(\frac{N_f}{N_{eq}}\right) = -\log\left[1 - \left(\frac{N_f}{N_{eq}}\right)^2\right] = \frac{\pi D_i t}{2.303 r^2} \quad (6)$$

where N_f and N_{eq} are amounts of uptake at time t and equilibrium, respectively; r is the particle radius. The diffusion coefficient D_i is calculated by using the values obtained from a cation-rich straight line of $-\log[1-(N_f - N_{eq})^2]$ versus t plot, were N_f and N_{eq} are uptakes at time t [18], for different concentrations and temperatures, D_i values are listed in Table 3 and shown in Fig. 7. The results

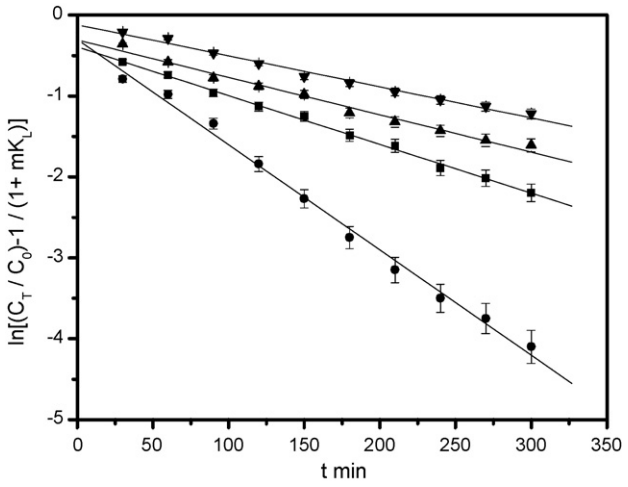

Fig. 6. Plots of $\ln[(C_t/C_e) - 1/(1+mK_L)]$ vs. time for the interactive effect of Pb(II) with 3.0 g dm^{-3} of Al/Zr-PILC$_{APT}$ clay (temperature of calcination = 723 K), at pH 6.0 and a controlled temperature of 298 ± 1 K for Pb(II) concentrations: 100.0 (●), 60.0 (■); 20.0 (▲) and 10.0 mmol dm^{-3} (▼).

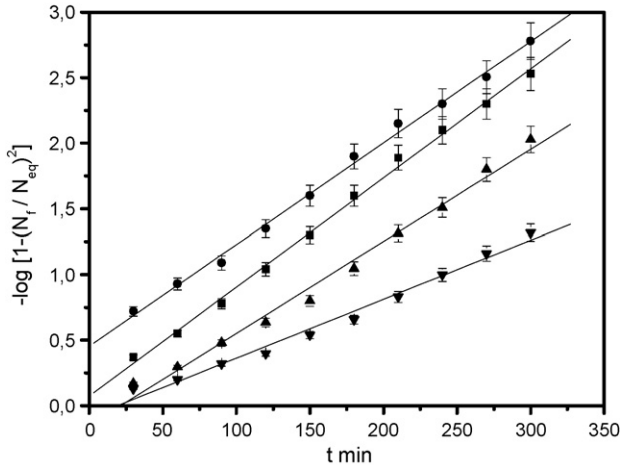

Fig. 7. Intraparticular mass transfer plots for adsorption onto 3.0 g dm^{-3} of Al/Zr-PILC$_{APT}$ clay (temperature of calcination = 723 K), at pH 6.0 and controlled temperature of 298 ± 1 K for Pb(II) concentrations: 100.0 (●), 60.0 (■); 20.0 (▲) and 10.0 mmol dm^{-3}(▼).

Table 4
Thermodynamic data for lead cation adsorption into natural and chemically modified smectite (clay 1.0 g dm^{-3}, 100.0 mg dm^{-3}, pH 6.0, time 700 min and controlled temperature in 298 ± 1 K)

Sample	N_f^{max} (mmol g^{-1})	b	N_s (mmol g^{-1})	$-\Delta$hint (Jg^{-1})	$-\Delta_{int}H^\circ$ (KJ mol^{-1})	$K_L \times 10^{-3}$	$-\Delta_{int}G^\circ$ (KJ mol^{-1})	$\Delta_{int}S^\circ$ (KJ mol^{-1})
CL	5.13 ± 0.15	6.05 ± 0.12	1.65 ± 0.13	13.71 ± 0.17	8.31 ± 0.15	9.99 ± 0.15	22.82 ± 0.17	48.69 ± 0.17
Al/Zr-PILC$_{APT-723}$	12.93 ± 0.11	12.61 ± 0.12	1.77 ± 0.13	14.64 ± 0.15	8.27 ± 0.15	14.58 ± 0.15	23.75 ± 0.17	51.95 ± 0.17
Al/Zr-PILC$_{APT-873}$	11.97 ± 0.13	11.59 ± 0.11	1.98 ± 0.13	16.06 ± 0.16	8.11 ± 0.15	14.06 ± 0.15	23.66 ± 0.17	52.18 ± 0.17

showed that D_i values increased significantly with decreasing initial Pb(II) concentrations. Decreasing the solute concentration in solution seems to reduce the diffusion of cations into the boundary layer and to enhance the diffusion into the mixed pillared and organofunctionalized surfaces.

The solid adsorption capacity for the lead halide by the modified smectite clay samples depend on the nature of the complex formed on the internal and external surface and external modified surface also on the affinity of the lead cation for the particular attached ligand [19,22] and number of reactive hydroxyl group and NH group anchored in the structure clay. The maximum adsorption capacity, N_f^{max}, for each lead halide through modified montmorillonite is listed in Table 4. It is observed that N_f^{max} is highest for lead cation for two modified matrixes.

3.3. Thermodynamic of adsorption

The thermostated solutions of the cations were incrementally added to the calorimetric vessel and the thermal effect of the titration $Q_t(J)$ was determined. Under the same experimental conditions, the corresponding thermal effect of the dilution of the cation solution was obtained in the absence of the support $Q_d(J)$. The thermal effect of the hydration of matrix in water was determined as before [23–34]. Under such conditions, the net thermal effect of adsorption $\Sigma Q_r(J)$ was obtained through Eq. (7).

$$\sum Q_r = \sum Q_t - \sum Q_d \quad (7)$$

The calorimetric results were presented in Fig. 8 and Table 4. The change in enthalpy associated with lead cation/natural and modified montmorillonite ($\Sigma\Delta_{int}h$) adsorption can be determined by modified Langmuir equation (Eq. (8)) [24]:

$$\frac{X}{\Delta_r h} = \frac{1}{(K_L - 1)\Delta_{int}h} + \frac{X}{\Delta_{int}h} \quad (8)$$

where X is the molar lead cation fractions remaining in solution. $\Delta_r h$ the enthalpy obtained from the quotient between the sums of the resulting effect per mass natural and modified smectite samples ($\Sigma Q_r h/m$), $\Delta_{int}h$ is the enthalpy for monolayer formation and K_L a parameter associated with the equilibrium constant. $\Delta_{int}h$ and K_L values can be determined from coefficients after linearization of the isotherm. The molar enthalpy of interaction process can be calculated through the Eq. (9) [25–34].

$$\Delta_{int}H = \frac{\Delta_{int}h}{N_s} \quad (9)$$

where N_s is the number of adsorbent moles after reaching calorimetric equilibrium. From K_L values the Gibbs energy is calculated by Eq. (10) [25–34]:

$$\Delta_{int}G = -RT \ln K_L \quad (10)$$

where K_L is the equilibrium constant obtained from Langmuir model, T the absolute temperature and the universal gas constant $R = 8.314 \times 10^{-3}$ kJ K^{-1} mol^{-1}, and enthalpy values by considering [25–34]:

$$\Delta_{int}G = \Delta_{int}H - T\Delta_{int}S \quad (11)$$

The resulting thermal effects due to the interaction of metals with natural and modified smectite samples are obtained by considering the deduction of dilution effect in water from the total thermal effect, applying Eq. (8).

The effect thermodynamic cycles for this series of intercalations involving a suspension (susp) of smectite samples (S) in aqueous (aq) solution with lead cation (Pb^{2+}) can be represented by the following calorimetric reactions [31,32]:

$$S(susp) + Pb^{2+}(aq) \rightarrow S{\cdot}Pb^{2+}(sup) \qquad Q_{tit} \quad (12)$$

$$S(susp) + nH_2O \rightarrow S{\cdot}nH_2O \qquad Q_{hit} \quad (13)$$

$$Pb^{2+}(aq) + nH_2O \rightarrow Pb^{2+}{\cdot}nH_2O(aq) \qquad Q_{dil} \quad (14)$$

$$S(sup) + Pb^{2+}(aq) \rightarrow S{\cdot}Pb^{2+} \qquad Q_r \quad (15)$$

The net thermal effect obtained for the calorimetric titration ($\Sigma Q_r = \Sigma Q_t - \Sigma Q_d$), as given by Eq. (15), was experimental represented as isotherms in Fig. 8a, In the Fig. 8b shows, as an example, one of the titration thermograms obtained by Al/Zr-PILC$_{APT-873}$

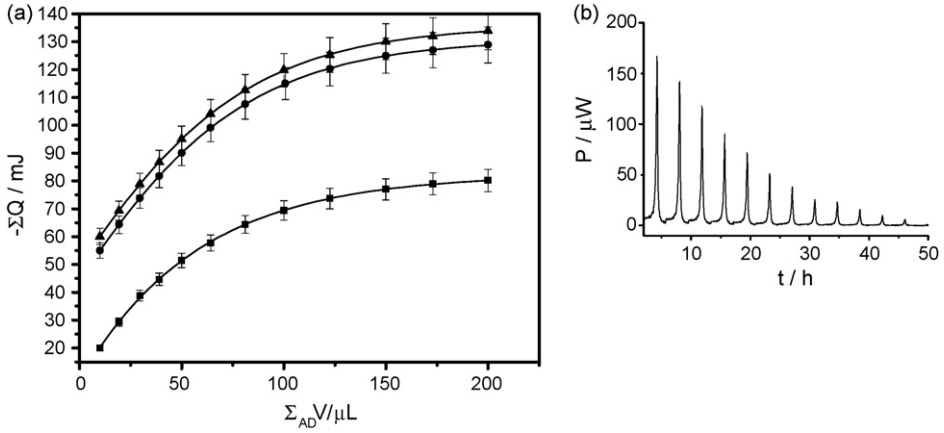

Fig. 8. The resulting thermal effects of the adsorption isotherms of the lead cation: CL (■), Al/Zr-PILC$_{APT-723}$ (▲), Al/Zr-PILC$_{APT-873}$ (●) (Pb(II) concentration 100.0 mmol dm^{-3}) (a) and variation of the power (heat flow) vs. time upon microcalorimetric titration of modified smectite (b).

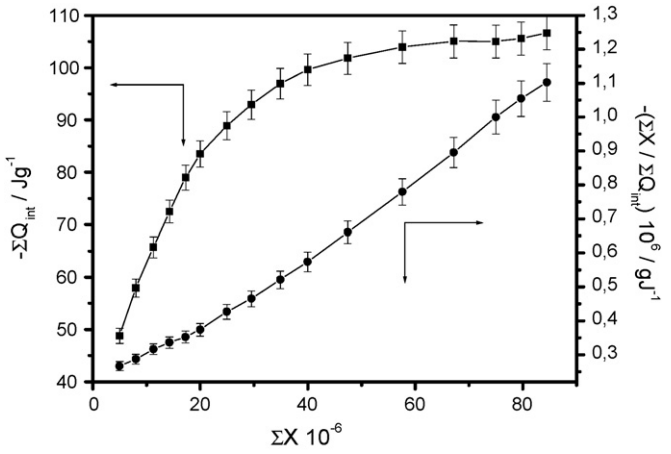

Fig. 9. Isotherm obtained from calorimetric titration of approximated 15.0 mg of intercalated smectite (Al/Zr-PILC$_{APT}$) suspended in water with 20.0 cm^{-3} of lead cation at 298 ± 1 K (Pb(II) concentration 100.0 mmol dm^{-3}) (■). This isotherm shows the integral enthalpy of adsorption vs. molar fraction. The straight line is the linearized form (●).

adsorbing Pb^{2+} cation: it evidences the fact that, under the present conditions, equilibrium is attained rapidly. The integrated heat value is obtained by use of the data treatment Digital 4.1 program (Thermometric).

One example of linearization involving lead cation adsorption is shown in Fig. 9. From Eq. (8) and linearized data for metallic divalent cation, the enthalpy ($\Delta_{int}H$) and entropy of interaction ($\Delta_{int}S$), can be obtained for all process, which enable calculation of molar enthalpy, Eq. (9). From the equilibrium constant the Gibbs free energy was calculated from Eq. (10) and combined with the enthalpic value, the entropy can also be calculated by Eq. (11).

The Gibbs free energy, entropy and enthalpy values are listed in Table 4. These values suggest that, during complex formation, the desolvation disturbs the structure of the reaction medium to promote the disorganization of the system and, consequently, leads to an increase in entropy [11]. The highest entropic values were observed for cation with the largest hydration volumes and illustrate the principle that the loss of waster of hydration leads to a disorganization of the final systems [25–34]. In conclusion, all thermodynamic values are favorable, with exothermic enthalpy, negative Gibbs free energy, and positive entropy, and corroborate lead cation/natural and modified smectite adsorption at the solid/liquid interface. According to the results obtained by Macedo et al. [34] in thermodynamic investigation with magadiite intercalated by *n*-alkydiamine. In this study the basic guest atom/silanol reactive center interactions inside the host nanospace gallery gave negative Gibbs free energy values. This set of data suggests spontaneity of these intercalation reactions.

4. Conclusions

The X-ray powder diffraction technique confirmed an expansion of the original smectites to thermally stable d_{001} spacing from 1.354 to 2.364 nm for Al/Zr-PILC$_{APT-723}$. For other clays the d_{001} peak proved the structural presence of pillars and APT ions in the matrices, which are stable to high temperatures of calcination, up to 873 K. These modified clays demonstrated an ability to adsorb Pb(II) cations from aqueous solutions.

The [3-(2-aminoethylamino)propyl]trimethoxysilane was successfully anchored onto the pillared smectite, new sites reactive were added in the clay surface through of the presence of the NH groups in agent intercalated chain. The process proceeded more effectively by evaporation of the solvent from dispersion of Al/Zr-PILC and xylene. APTS was intercalated directly into structure of intercalated pillared clay with Al/Zr and silylated with silanol group, resulting in the grafting of APTS on internal, external smectite surface and external part of pillars.

The kinetic studies demonstrated an equilibrium time of 700 min for Pb(II) adsorption on modified materials and the experimental data was correlated by external mass transfer diffusion for the first stage and intraparticle mass transfer diffusion models for the second stage of adsorptions.

The quantitative interaction lead cation/basic reactive centers (OH and NH) of chemically modified smectite were followed calorimetrically at the solid/liquid interface to give favorable sets of thermodynamic data, such as exothermic enthalpy, negative Gibbs free energy, and positive entropic values.

Acknowledgements

The authors are indebted to CNPq (P.n. 150060/2006-8) for fellowships and FAPESP for financial support.

References

[1] T.J. Pinnavaia, M. Tzou, S.D. Landau, On the pillaring and delamination of smectite clay catalysts by polyoxo cations of aluminum, J. Mol. Catal. 27 (1984) 195–212.
[2] D.L. Guerra, V.P. Lemos, C. Airoldi, R.S. Angélica, Influence of the acid activation of pillared smectites from Amazon (Brazil) in adsorption process with butylamine, Polyhedron 25 (2006) 2880–2890.
[3] D.L. Guerra, C. Airoldi, R.R. Viana, Performance of modified montmorillonite clay in mercury adsorption process and thermodynamic studies, Inorg. Chem. Commun. 11 (2008) 20–24.
[4] C. Volzone, Pillaring of different smectite members by chromium species (Cr-PILCs), Microporous Mesoporous Mater. 49 (2001) 197–202.
[5] A. Gil, M.A. Vicente, L.M. Gandia, Main factors controlling the texture of zirconia and alumina pillared clays, Microporous Mesopororous Mater. 34 (2000) 115–125.
[6] J.L. Valverde, P. Sanchez, F. Dorado, C.B. Molina, A. Romero, Influence of the synthesis conditions on the preparation of titanium-pillared clays using hydrolyzed titanium ethoxide as the pillaring agent, Microporous Mesoporous Mater. 54 (2003) 155–165.
[7] M. Alkan, S. Çelikçapa, Ö. Demibaş, M. Doğan, Removal of reactive blue 221 and acid blue 62 anionic dyes from aqueous solutions by sepiolita, J. Colloid Interface Sci. 65 (2005) 251–259.
[8] R. Petschick, G. Kuhn, F. Gingele, Clay minerals distribution surface sediments of the south Atlantic: sources, transport and relation to oceanography, Mar. Geol. 130 (1996) 203–229.
[9] D.M. Moore, R.C. Reynolds Jr., X-ray Diffraction and the Identification and Analysis of Clay Minerals, second ed., Oxford University Press, Oxford, 1997.
[10] H. Shizozu, Introduction to Clay Mineralogy-Fundamentals for Clay Science, Asakura Publication, Japan, 1988.
[11] K.G. Bhattacharyya, S.S. Gupta, Pb(II) uptake by kaolinite and montmorillonite in aqueous medium: influence of activation of the clays, Colloids Surf., A 277 (2006) 191–200.
[12] M.R. Sun Kou, S. Mendioroz, M.L. Guijarro, A thermal study of Zr-pillared montmorillonite, Thermochim. Acta 323 (1998) 142–157.
[13] M.L. Menezes, J.C. Moreira, J.T.S. Campos, Adsorption of various ions from acetone and ethanol on silica gel modified with 2-, 3-, and 4-aminobenzoate, J. Colloid Interface Sci. 179 (1996) 207–210.
[14] C. Airoldi, M.O. Machado, A.M. Lazarin, Thermodynamic features associated with intercalation of some *n*-alkylmonoamines into barium phosphate, J. Chem. Thermodyn. 38 (2006) 130–135.
[15] A.R. Thompson, R.E. Botto, NMR of layered silicates in argonne coals and geochemical implications, Energy Fuels 15 (2001) 176–181.
[16] K.W. Park, O.Y. Kwon, Interlamellar silylation of montmorillonite with 3-Aminopropyltriethoxysilane, Bull. Korean Chem. Soc. 25 (2004) 965–968.
[17] Y.S. Ho, G. McKay, A kinetic study of Dye Sorption by biosorbent waste product pith, Resour. Conserv. Recycl. 25 (1999) 171–193.
[18] G. Mckay, M.J. Bino, A. Altememi, External mass transfer during the adsorption of various pollutants onto activated carbon, Water Res. 20 (1986) 432–435.
[19] D.M. Manohar, B.F. Noeline, T.S. Anirudhan, Adsorption performance Al-pillared betonite clay for the removal of cobalt (II) from aqueous phase, Appl. Clay Sci. 31 (2006) 194–206.
[20] J. Tunney, C. Detellier, Preparation and characterization of two distinct ethylene glycol derivatives of kaolinite, Clays Clay Miner. 42 (1994) 552–560.
[21] K. Urano, H. Tachikawa, Process development for removal and recovery of phosphorus from wastewater by a new adsorbent. 1. Preparation method and adsorption capability of a new adsorbent, Ind. Eng. Chem. Res. 2 (1991) 30–35.

[22] M.A. Schlautman, J.J. Morgan, Adsorption of aquatic humic substances on colloidal-size aluminum oxide particles: influence of solution chemistry, Geochim. Cosmochim. Acta 58 (1994) 4293–4303.
[23] A.G.S. Prado, C. Airoldi, Adsorption preconcentration and separation of cations on silica gel chemically modified with the herbicide 2,4-dichlorophenoxyacetic acid, Anal. Chim. Acta 432 (2001) 201–211.
[24] R.S.A. Machado, M.G. Fonseca, L.N.H. Arakaki, S.F. Oliveira, Silica gel containing sulfur, nitrogen and oxygen as adsorbent centers on surface for removing copper from aqueous/ethanolic solutions, Talanta 63 (2004) 317–322.
[25] A.M. Lazarin, C. Airoldi, Thermochemistry of intercalation of *n*-alkylmonoamines into lamellar hydrated barium phenylarsonate, Thermochim. Acta 454 (2007) 43–49.
[26] V.S.O. Ruiz, C. Airoldi, Thermochemical data for *n*-alkylmonoamine intercalation into crystalline lamellar zirconium phenylphosphonate, Thermochim. Acta 420 (2004) 73–78.
[27] O.A.C. Monteiro, C. Airoldi, The influence of chitosans with defined degrees of acetylation on the thermodynamic data for copper coordination, J. Colloid Interface Sci. 282 (2005) 32–37.
[28] Z. Aksu, Determination of equilibrium, kinetic and thermodynamic parameters of the batch biosorption of Niquel(II) ions onto Chlorella vulgaris, Process Biochem. 38 (2002) 89–99.
[29] P.D. Padilha, J.C. Rocha, J.C. Moreira, J.T.D. Campos, C.D. Federici, Preconcentration of heavy metals ions from aqueous solutions by means of cellulose phosphate: an application in water analysis, Talanta 45 (1997) 317–323.
[30] M.G. Fonseca, C. Airoldi, Action of silylating agents on a chrysotile surface and subsequent reactions with 2-pyridine and 2-thiophene carbaldehydes, J. Chem. Soc., Dalton Trans. 42 (1999) 3687–3692.
[31] A.I. Martin, M. Sanchez-Chaves, F. Arranz, Synthesis, characterization and controlled release behaviour of adducts from chloroacetylated cellulose and α-naphthylacetic acid, React. Funct. Polym. 39 (1999) 179–187.
[32] C. Airoldi, J. Sales, F. Farias, A. Prado, Attachment of 2-aminomethylpyridine molecule onto grafted silica gel surface and its ability in chelating cations, Polyhedron 23 (2004) 719–725.
[33] C. Airoldi, A. Tosta, A. Prado, Adsorption, separation, and thermochemical data on the herbicide picloram anchored on silica gel and its cation interaction behavior, J. Colloid Interface Sci. 269 (2004) 259–264.
[34] T.R. Macedo, G.C. Petrucelli, C. Airoldi, Silicic acid magadiite guest molecules and features related to the thermodynamics of intercalation, Clay Clay Miner. 55 (2007) 151–159.